

# REQUIREMENTS AND RESULTS FOR QUADRUPOLE MODE MEASUREMENTS

Adrian Oeftiger\*, CERN, Geneva, Switzerland

## Abstract

Direct space charge may be quantified, and hence the beam brightness observed, by measuring the quadrupolar beam modes in the CERN Proton Synchrotron (PS). The spectrum of the transverse beam size oscillations (i.e. the quadrupolar beam moment) contains valuable information: the betatron envelope modes and the coherent dispersive mode indicate optics mismatch, while their frequency shifts due to space charge allow a direct measurement thereof. To measure the quadrupolar beam moment we use the Base-Band Q-meter system of the PS which is based on a four electrode stripline pick-up. Past experiments with quadrupolar pick-ups often investigated coasting beams, where the coherent betatron and dispersion modes correspond to single peaks in the tune spectrum. In contrast, long bunched beams feature bands of betatron modes: the mode frequencies shift depending on the transverse space charge strength which varies with the local line charge density. By using the new transverse feedback (TFB) in the PS as a quadrupolar RF exciter, we measured the quadrupolar beam transfer function. The beam response reveals the distinct band structure of the envelope modes as well as the coherent dispersive mode.

## INTRODUCTION

The transverse second-order moments of a beam distribution can be measured with the aid of sensitive quadrupolar pick-ups (QPU) featuring four electrodes in quadrupolar configuration. In particular under stable beam conditions, the oscillations about the matched beam values can give insight on transverse emittances, optics mismatch, and space charge strength. Our measurements with the QPU at the CERN Proton Synchrotron aim to characterise the new high brightness beams in the context of the LHC Injector Upgrade [1]. The goal is to establish a direct experimental method to assess space charge strength, which can also be used to benchmark advanced numerical simulation set-ups.

In the past, QPU studies have been conducted both in the time domain (fitting the quadrupole moment for emittance measurements, cf. [2, 3]) and more often in the frequency domain. The frequency domain is advantageous in the sense that the oscillatory or differential signal content is much less noise affected than the absolute signal values. Beam frequency response measurements have been used e.g. for emittance measurements [4], while space charge studies cover the majority of QPU studies [5–8].

The CERN PS provides good experimental conditions to establish the method enabling us to study various space charge strengths and tune coupling conditions. The present hardware includes the new transverse feedback system which

we exploit to measure the quadrupolar beam transfer function in order to characterise the quadrupolar eigenmodes. The planned upgrades of the BBQ systems in the PS Booster and the Super Proton Synchrotron will extend the availability of quadrupolar moment measurements to these machines.

This paper first reviews the theoretical basics yielding the expressions for modes of quadrupolar order. We employ the smooth approximation where not explicitly stated otherwise, i.e. the lattice functions remain constant along the ring. A more comprehensive overview of most of the derivations and arguments is given in Ref. [9, chapter 2]. The next section describes the experimental set-up for the quadrupolar beam transfer function measurement in the CERN PS and presents the measured beam frequency response. Eventually, these results are briefly compared to numerical simulations carried out with PyHEADTAIL [10] using a self-consistent 3D space charge model [11].

## THEORETICAL CONSIDERATIONS

Let  $\zeta \doteq (x, y, z, x', y', \delta)$  denote the vector of the six phase space coordinates of the beam particles. The spatial coordinates  $x$  and  $y$  measure the horizontal and vertical displacement from the orbit, while  $z$  indicates the longitudinal spatial displacement from the RF wave's zero crossing. The canonical momenta  $p_x, p_y, p_z$  are embedded in  $x' \doteq p_x/p_0$ ,  $y' \doteq p_y/p_0$  and  $\delta = (p_z - p_0)/p_0$  while the beam momentum  $p_0 = \beta\gamma m_p c$  is considered constant, denoting with  $\beta$  the beam speed in units of speed of light  $c$ , with  $\gamma$  the relativistic Lorentz factor of the beam and with  $m_p$  the mass per particle.

It is well known that in a coasting beam with a transverse uniform Kapchinskij-Vladimirskij (KV) distribution [12], the particles oscillate at one single incoherent tune. The defocusing nature of transverse space charge translates to the incoherent tune being negatively shifted from the bare machine tune. This KV tune shift is frequently used as a unit to express the strength of space charge in a machine, it amounts to

$$\Delta Q_{x,y}^{KV} = -\frac{K^{SC} R^2}{4\sigma_{x,y}(\sigma_x + \sigma_y)Q_{x,y}}, \quad (1)$$

where  $R$  denotes the effective machine radius,  $\sigma_{x,y}$  the transverse r.m.s. beam sizes and  $Q_{x,y}$  the transverse bare machine tunes. The dimensionless space charge perveance reads

$$K^{SC} \doteq \frac{q\lambda}{2\pi\epsilon_0\beta\gamma^2 p_0 c} \quad (2)$$

with  $q$  the charge per particle,  $\lambda$  the line charge density in C/m and  $\epsilon_0$  the vacuum permittivity.

If the beam is transversely Gaussian normal distributed, space charge becomes non-linear. The linearised slope of

\* adrian.oeftiger@cern.ch

Content from this work may be used under the terms of the CC BY 3.0 licence (© 2018). Any distribution of this work must maintain attribution to the author(s), title of the work, publisher, and DOI.

the self-fields in the core of the Gaussian distribution then amounts to twice the linear slope of the *r.m.s.-equivalent* KV distribution. On the other hand, space charge becomes very weak for the halo particles far outside the core. Therefore, the space charge shifted incoherent tunes  $\Delta Q_{x,y}^{SC}$  spread from close to the bare betatron tune  $Q_{x,y}$  to twice the KV incoherent tune shift:

$$\max \{ \Delta Q_{x,y}^{SC} \} = 2 \cdot \Delta Q_{x,y}^{KV} \quad (3)$$

In terms of the coherent perspective, the transverse dipolar moments of the beam distribution  $f$ ,

$$\langle u \rangle(s) = \int d^6 \zeta u f(\zeta; s) \quad (4)$$

for  $u = x, y$  and  $s$  the path length along the ring, remain unaffected by space charge: due to Newton's principle of *actio = reactio*, the sum of all binary forces between the particles vanishes. Direct space charge hence plays a role only from the quadrupolar moments on,

$$\sigma_u(s) = \int d^6 \zeta (u - \langle u \rangle)^2 f(\zeta; s) \quad (5)$$

In the transverse plane, the quadrupolar moments are often referred to as envelopes. Assuming beams of elliptic symmetry with a monotonically decreasing distribution within a constant focusing channel with decoupled optics, the *r.m.s.* envelope equations [12, 13] describe the evolution of these quadrupolar moments  $\sigma_{x,y}(s)$  along the ring,

$$\begin{aligned} \frac{d^2 \sigma_x}{ds^2} + K_x \sigma_x - \frac{\epsilon_{x,geo}^2}{\sigma_x^3} - \frac{K^{SC}}{2(\sigma_x + \sigma_y)} &= 0 \\ \frac{d^2 \sigma_y}{ds^2} + K_y \sigma_y - \frac{\epsilon_{y,geo}^2}{\sigma_y^3} - \frac{K^{SC}}{2(\sigma_x + \sigma_y)} &= 0 \end{aligned} \quad (6)$$

Here,  $K_{x,y} = (\beta_{x,y})^{-2} = (Q_{x,y}/R)^2$  represent the external focusing in each plane with  $\beta_{x,y}$  denoting the constant betatron functions. The (possibly slowly changing) geometric transverse emittances  $\epsilon_{\{x,y\},geo}$  provide the respective thermal barrier term. Last but not least, the space charge perveance term couples the two envelope equations.

By linearising Eq. (6) around the equilibrium values of the quadrupolar moments, one can solve the corresponding eigenvalue problem. Under stable beam conditions (e.g. neglecting modes that can change the emittance) one finds two quadrupolar eigenmodes of the envelope equations at the two tunes  $Q_{\pm}$ . In their expressions (see e.g. Ref. [9, Eq. (2.110)]) one readily finds a term proportional to the expression of the incoherent KV tune shift Eq. (1). After substituting this term and neglecting quadratic orders, one readily derives the general relation

$$\Delta Q_{x,y}^{KV} = \frac{1 + \frac{\sigma_{y,x}}{\sigma_{x,y}}}{2Q_{x,y}} \Lambda \quad (7)$$

where the physical observables (i.e. the quadrupolar modes  $Q_{\pm}$ , bare machine tunes  $Q_{x,y}$  and the beam size ratio  $\sigma_y/\sigma_x$ )

are explicitly contained in the quantity

$$\Lambda \doteq \frac{Q_+^2 + Q_-^2 - 4 [Q_x^2 + Q_y^2]}{4 + 3 \frac{\sigma_y}{\sigma_x} + 3 \frac{\sigma_x}{\sigma_y}} \quad (8)$$

$\Lambda$  is negative (such as  $\Delta Q_{x,y}^{KV}$ ) which reflects the defocusing effect of direct transverse space charge. The general expression Eq. (7) for the quadrupolar modes (first derived in [14]) has two well-known limit cases:

1. the decoupled split tunes case (e.g. [5, first Eq.]) with independent horizontal and vertical mode, and
2. the fully coupled axi-symmetric case (e.g. [15, Eqs. (26) and (28)]) with the anti-symmetric and the breathing mode.

Equation (7) in principle allows to measure the strength of space charge (in units of the KV tune shift) directly through the observation of the quadrupolar frequencies. Reference [16] discusses how approaching the coupling resonance reflects on the KV tune shift when comparing to the decoupled split tunes formula.

The power of the envelope equations lies in the *r.m.s.-equivalence* of beam distributions, whose collective second-order dynamics are uniquely described by Eq. (6) [13, 15, 17]. Suppose two different transverse distributions of the same *r.m.s.* sizes (e.g. the above Gaussian and KV distribution): even though the incoherent tunes may be distributed very differently, the coherent behaviour of these two *r.m.s.-equivalent* beams under space charge will be identical.

Until here we have discussed coasting beam conditions. Under typical synchrotron conditions, longitudinal motion is orders of magnitude slower than the transverse particle oscillations. This variation in bunched beams can hence be considered adiabatic, which leads to longitudinally varying space charge conditions for the transverse beam dynamics. In the incoherent picture, the above space charge tune shift Eq. (1) then effectively scales with  $\Delta Q_{x,y}^{KV} = \Delta Q_{x,y}^{KV}(z) \propto \lambda(z)$ . Ref. [6] discusses the corresponding implications for the collective motion by investigating the three-dimensional envelope equations including the longitudinal  $\sigma_z$  envelope. For long bunches and low synchrotron frequency, the transverse and longitudinal degrees of freedom indeed decouple resulting in coasting beam like conditions for the transverse plane, cf. e.g. [6, Fig. 2]. Consequently, the transverse quadrupolar modes remain well described by the previous two-dimensional expressions, which now depend on the varying longitudinal line charge density  $\lambda(z)$ . Considering the quadrupolar frequency spectrum for a typical parabolic bunch shape, one therefore now expects two *bands of envelope modes*, one for the higher  $Q_+(z)$  and one for the lower  $Q_-(z)$  (which can in principle overlap for strong space charge). Each band ranges from the vanishing space charge conditions at the head and tail of the bunch to the strongest transverse self-fields at the bunch core. The former condition leaves  $Q_{\pm}$  close to  $2Q_{x,y}$  while the latter translates to maximally reduced  $Q_{\pm}$ . This *coherent* tune spread of

the envelopes due to the longitudinal bunch profile should not be confused with the *incoherent* tune spread of a transverse non-uniform distribution (such as the aforementioned Gaussian normal distribution).

In the case of linear coupling (through skew quadrupole components in the external magnetic fields), additional  $K_{xy}\sigma_{x,y}$  coupling terms enter the envelope equations Eq. (6). This system of equations has been solved in Ref. [18] and two additional distinct odd modes are found (again restricting ourselves to stable beam conditions). For vanishing space charge, the two even quadrupolar modes  $Q_{\pm}$  reduce to  $2Q_x$  and  $2Q_y$ , while the two odd modes essentially reduce to  $|Q_x - Q_y|$  and  $|Q_x + Q_y|$ .

One more important ingredient to understand the eigenmodes within the quadrupolar spectrum of a beam with finite momentum spread is due to the dispersion function  $D_x$  generated by the horizontal bending magnets in a planar circular machine. With the dispersive contribution to the horizontal r.m.s. beam size,

$$\sigma_x^2 = \beta_x \epsilon_{x,\text{geo}} + D_x^2 \delta^2 \quad , \quad (9)$$

the set of coasting-beam envelope equations Eq. (6) correspondingly extends to a third equation for the dispersion function modified by space charge [19, 20]. This additional degree of freedom gives rise to yet another second-order eigenmode, the *coherent dispersion mode*. At zero current and no synchrotron motion, its tune  $Q_d$  is identical to the horizontal bare tune  $Q_x$ , while  $Q_d$  decreases with increasing space charge.

## MEASUREMENTS

### Set-up

In the PS, the stripline pick-up PR.BQL72 in section 72 is part of the base-band Q-measurement (BBQ) system. For our measurements, the four electrodes top (T), bottom (B), left (L) and right (R) are configured in quadrupolar mode yielding the following combined signal of induced voltages,

$$V_q = (V_L + V_R) - (V_T + V_B) \quad . \quad (10)$$

This combination results in the QPU time signal for the  $k$ th turn

$$\begin{aligned} S_{\text{QPU}}(k) &\propto \langle x^2 \rangle - \langle y^2 \rangle \\ &= \sigma_x^2(k) - \sigma_y^2(k) + \langle x \rangle^2(k) - \langle y \rangle^2(k) \quad , \quad (11) \end{aligned}$$

where  $\langle \cdot \rangle$  refers to the integration over phase space  $\int d^6 \zeta f(\zeta; k)$ . Analogous to the set-up in [8], we are mainly interested in the frequency content of this signal in order to determine the quadrupolar eigenmodes of the proton beam. To this end, summation and subtraction of the induced electrode potentials are carried out in analog. Only then is the result digitised in order to improve the resolution of the generally very small quadrupolar signal amplitudes.

In order to measure the quadrupolar beam transfer function, we excite the beam via the kicker plates of the new TFB

system of the PSB in section 97. First, the orbit has been corrected to minimise the induced difference signal on the kicker plates. To increase the sensitivity, the 20 dB attenuators between the plate signals and the read-out electronics have been removed. The centred orbit should suppress dipolar feed-down of the quadrupolar excitation.

When pulsing the RF quadrupole at revolution frequency, i.e.  $h = 1$ , it acts like an additional static quadrupolar field to the beam. We characterised the strength of this RF quadrupole by measuring the tune difference comparing between no voltage and maximum amplitude (i.e. an input signal before the amplifier of 1 V peak-to-peak). The dipolar tunes have been determined by mixing all 43 BPM positions per plane [21] and evaluate the assembled signal via SUSSIX frequency analysis [22]. When scanning the relative phase between the RF quadrupole and the beam, we found a statistically significant maximum tune difference of  $\Delta Q_x = 3 \times 10^{-3}$  and  $\Delta Q_y = 2 \times 10^{-3}$ .

This is a significant static impact on the beam, leading to the conclusion that the TFB in quadrupolar configuration should indeed be strong enough to resonantly excite the quadrupolar beam eigenmodes at the respective frequencies.

For the quadrupolar beam transfer function measurement, we start from a nominal LHC25 beam preparation cycle set-up in the PS. In the upstream injector, the Booster, the beams are prepared with a longitudinal acceptance bottleneck (equivalently to LHCINDIV beams) in order to achieve large transverse emittances and low intensities. The machine and beam parameters have been summarised in Table 1. The KV tune shift of the operational LHC25 beams is about a factor 5 higher (fivefold bunch intensity at roughly the same transverse emittance).

Table 1: PS Machine and Beam Parameters

Lorentz factor PS injection	$\gamma = 2.49$
revolution frequency	$f_{\text{rev}} = 437 \text{ kHz}$
beam intensity	$N = 0.3 \times 10^{12} \text{ ppb}$
number of bunches stored	1
transverse emittance	$\epsilon_{x,y} = 2.3 \text{ mm mrad}$
average betatron function	$\beta_x \approx \beta_y \approx 16 \text{ m}$
average dispersion	$D_x \approx 3 \text{ m}$
r.m.s. momentum deviation	$\sigma_\delta = 1 \times 10^{-3}$
bunch length	$B_L = 180 \text{ ns}$
synchrotron tune	$Q_s = 1.67 \times 10^{-3}$
KV space charge tune shift	$\Delta Q_{x,y}^{\text{KV}} = 0.02$

In the PS, usually the skew quadrupole magnets are powered as to provide strong linear coupling in the optics in order to suppress horizontal head-tail instabilities [23]. We removed the linear coupling globally within a small time window of 15 ms during the cycle by adjusting the skew quadrupole components using the closest tune approach [24]. During 12 ms of this window the TFB has been pulsed

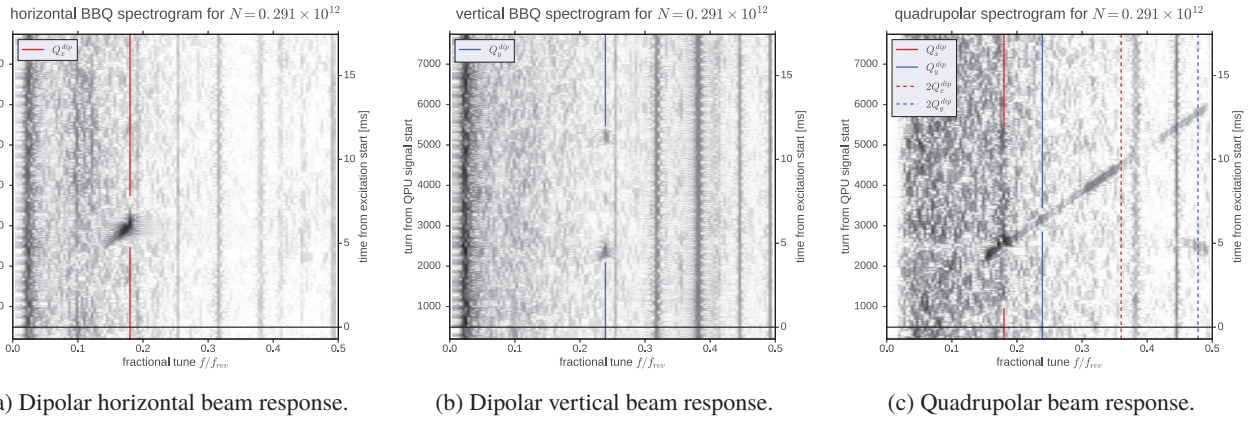


Figure 1: Spectrograms of dipolar BQS69 signals and the quadrupolar BQL72 signal.

in quadrupolar mode by means of an external waveform generator: its excitation signal was split for each transverse plane with one of the two channels inverted, amplified and eventually fed to the kicker plates. As the hybrid splitter and inverter were limited to RF above 2 MHz, we chirped between 2.19 MHz to 2.4 MHz corresponding to harmonic  $5.01 \leq h \leq 5.49$ . This swept frequency range covers all relevant quadrupolar eigenmodes for bare machine tunes below a fractional tune of  $q_{x,y} \leq 0.25$ . In principle, quadrupolar excitation at beam eigenfrequencies directly results in emittance growth – thus, the frequency sweep needs to be fast enough to treat this chirp as a mere perturbation to the beam. We ensured the validity of this assumption by comparing flying wire scan profiles before and after the excitation indicating negligible transverse r.m.s. emittance growth,  $\Delta\epsilon_{x,y}/\epsilon_{x,y} \leq 5\%$ .

## Results

Along with the quadrupolar  $S_{QPU}$  signal we also recorded the dipolar signals from the shoe-box pick-up BQS69 with an optimised linear response. Figure 1 presents spectrograms of the corresponding dipolar and quadrupolar turn-by-turn data based on a 256 turn sliding FFT window. Figs. 1a and 1b show the tunes  $Q_x, Q_y$  as dipolar beam eigenmodes for the horizontal and vertical plane, respectively. Tune shifts from impedances and indirect space charge are of the order  $O(10^{-3})$  [25], such that for the present low beam intensities the measured dipolar tunes do not differ significantly from the bare machine tunes. The quadrupolar signal  $S_{QPU}$  during the excitation is shown in Fig. 1c: note the two envelope bands below  $2Q_x, 2Q_y$  which are absent in the dipolar spectra. The two instrumentation-based frequencies  $0.381f_{rev}$  and  $0.445f_{rev}$  are beam independent and are ignored here (similar irrelevant constant frequency lines exist in the dipolar spectra).

The turn where  $S_{QPU}(k)$  maximally correlates with the reconstructed chirp excitation signal  $I_{exc}(k)$  yields the start of excitation. The sinusoidal beam response contained in  $S_{QPU}$  can be interpreted like a modulation of the original excitation signal, in analogy to radio signal as a modulation

on top of a baseband frequency. Demodulation of  $S_{QPU}(k)$  with the zero-padded  $S_{exc}(k)$  and its  $90^\circ$  shifted quadrature signal  $C_{exc}(k)$  (which can be obtained e.g. by a Hilbert filter) gives the in-phase  $I$  and quadrature  $Q$  components of the beam response,

$$I(k) = S_{QPU}(k) \cdot S_{exc}(k) \quad (12)$$

$$Q(k) = S_{QPU}(k) \cdot C_{exc}(k) \quad (13)$$

Filtering  $I$  and  $Q$  with a triangular Savitzky-Golay low-pass filter of 65 turns width then extracts the pure beam response content around the excitation baseband. Plotting the filtered amplitude  $\sqrt{I^2 + Q^2}$  vs. the instantaneous excitation frequency  $f_{exc}(k)$  yields the frequency response of the beam, which is depicted in Fig. 2. The two envelope bands are

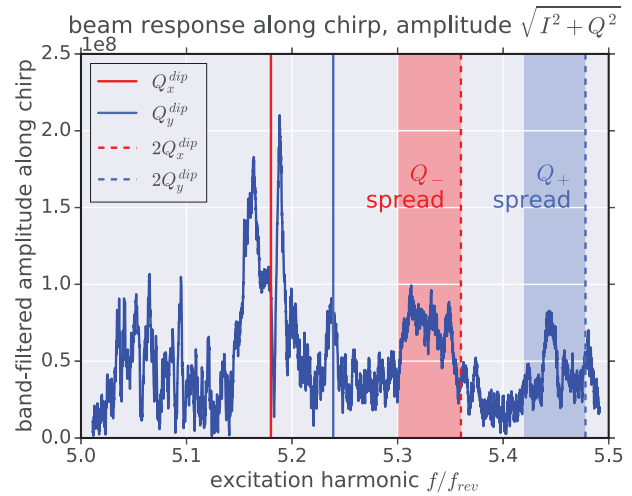


Figure 2: Demodulated frequency response of the beam.

indicated by “ $Q_{\pm}$  spread”. The colour areas mark their estimated extents below the measured dipolar tunes  $2Q_{x,y}$  of about

$$\Delta Q_{+} \approx 0.058 \quad \text{and} \quad \Delta Q_{-} \approx 0.06 \quad (14)$$

Under the assumption that only direct space charge contributes to the envelope spread, applying Eq. (6) to these

values and the beam parameters of Table 1 yields KV tune shifts of  $\Delta Q_x^{KV} \approx 0.05$  and  $\Delta Q_y^{KV} \approx 0.04$  – twice as much as the computed value in Table 1 based on Eq. (1).

The beam response shows the dipolar peaks at  $Q_y$  and with small amplitude at  $Q_x$ . The latter is neighboured by a large and wide peak on the left and a narrow peak on the right. The left peak is a candidate for the coherent dispersive mode shifted downwards from  $Q_x$  by space charge.

## NUMERICAL SIMULATIONS

PyHEADTAIL Simulations on the GPU with a 3D particle-in-cell space charge model yield the quadrupolar eigenmodes of the PS bunch. The macro-particle simulations are based on linear betatron motion in a constant focusing channel with non-linear synchrotron motion. Without taking into account dispersion and chromaticity, the simulated quadrupolar spectrum exhibits envelope bands whose width identically reproduces Eq. (7). When including effective dispersion at  $D_x = 3$  m, the coherent dispersive mode enters the spectrum as a distinct peak located at  $Q_x$ . Increasing the synchrotron tune for vanishing space charge shows that the coherent dispersive mode splits into two peaks at  $Q_x \pm Q_s$ . This separation almost vanishes for the usual PS conditions at  $Q_s = 0.0017$ , cf. Table 1. For finite space charge, the coherent dispersive mode indeed shifts below  $Q_x$  as explained in the theory section. However, only including the natural linear chromaticity of the PS,  $Q'_x = -0.83Q_x$  and  $Q'_y = -1.12Q_y$ , recovers the measured location of the coherent dispersive mode. Most importantly, chromaticity effectively broadens the width of the envelope bands to almost twice the value as observed without chromaticity. Figure 3 compares these simulation results for the  $\sigma_x^2 - \sigma_y^2$  signal (without the dipolar contributions) to the measured beam frequency response. Applying SUSSIX frequency analysis reveals the contained side-band structure proving the influence of the longitudinal plane: the coherent dispersive mode splits into several peaks in distance of  $Q_s$  and the same happens to the envelope bands.

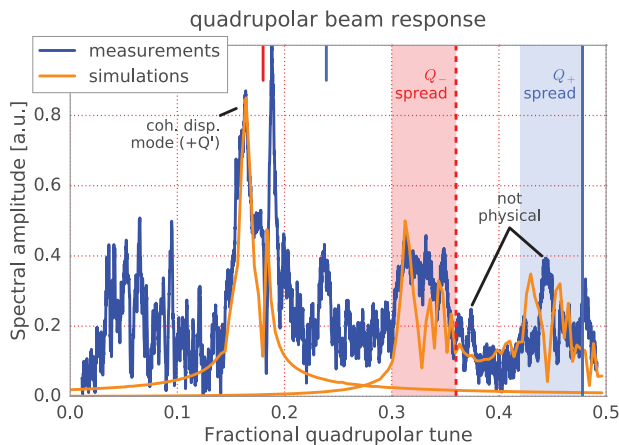


Figure 3: Comparison between measured beam frequency response and simulated eigenmodes.

## CONCLUSION

This paper presented the direct measurement technique of space charge in units of the incoherent KV tune shift via the corresponding frequency shift of coherent quadrupolar i.e. second-order modes. The measured quadrupolar frequency response of bunched beam at the CERN PS shows the expected envelope bands. This clearly qualifies the PS hardware equipment: the kicker plates of the PS transverse feedback system in quadrupolar configuration sufficiently excite the beam to observe the typically rather weak envelope eigenmodes by the stripline pick-up, which thus proves to be sensitive enough. Furthermore, the second-order coherent dispersive mode has been identified as a significant spectral component. The comparison of the measurements with numerical simulations points out chromaticity as a major impact: finite chromaticity considerably modifies the quadrupolar eigenmodes by (i.) broadening the envelope bands and (ii.) splitting the coherent dispersive mode into side-bands. The former observation has necessarily to be taken into account when inferring the incoherent KV tune shift from the envelope band width.

Next steps for the on-going CERN studies include (i.) quadrupolar beam transfer function measurements at vanishing chromaticity, (ii.) further investigation of injection oscillations, in particular Chernin's odd envelope modes when injecting from decoupled transfer line optics into tightly coupled PS optics, and (iii.) dedicated space charge experiments such as resonance studies. A theoretical analysis of quadrupolar modes at finite linear chromaticity could vastly improve the present understanding, which to the knowledge of the author has so far not been investigated.

## ACKNOWLEDGEMENTS

The author would like to thank Simon Albright, Heiko Damerau, Elias Métral, Guido Sterbini, Malte Titze and Panagiotis Zisopoulos for fruitful discussions as well as Marek Gasior, Tom Levens and Marcel Coly for their kind technical support. Research supported by the HL-LHC project.

## REFERENCES

- [1] H. Damerou *et al.*, “LHC Injectors Upgrade, Technical Design Report, Vol. I: Protons,” Tech. Rep. CERN-ACC-2014-0337, Dec. 2014.
- [2] R. H. Miller, J. E. Clendenin, M. B. James, and J. C. Shepard, “Nonintercepting emittance monitor,” Stanford Linear Accelerator Center, Tech. Rep., 1983.
- [3] A. Jansson, “Noninvasive single-bunch matching and emittance monitor,” *Physical Review Special Topics-Accelerators and Beams*, vol. 5, no. 7, p. 072 803, 2002.
- [4] C.-Y. Tan, “Using the quadrupole moment frequency response of bunched beam to measure its transverse emittance,” Fermi National Accelerator Laboratory (FNAL), Batavia, IL, Tech. Rep., 2007.
- [5] M. Chanel, “Study of beam envelope oscillations by measuring the beam transfer function with quadrupolar pick-up and kicker,” in *European Particle Accelerator Conference (EPAC 1996)*, 1996, pp. 1015–1017.
- [6] T. Uesugi *et al.*, “Observation Of Quadrupole Mode Frequency And Its Connection With Beam Loss,” no. KEK-99-98, 1999.
- [7] R. C. Bär, “Untersuchung der quadrupolaren btf-methode zur diagnose intensiver ionenstrahlen,” Universität Frankfurt, Germany, 2000.
- [8] R. Singh *et al.*, “Observations of the quadrupolar oscillations at gsi sis-18,” in *International Beam Instrumentation Conference*, 2014.
- [9] A. Oeftiger, “Space Charge Effects and Advanced Modelling for CERN Low Energy Machines,” PhD thesis at EPFL, Lausanne, Switzerland, 2016.
- [10] K. Li *et al.*, “Code development for collective effects,” no. CERN-ACC-NOTE-2017-0008, WEAM3X01. 7 p, Jul. 2016.
- [11] A. Oeftiger and S. E. Hegglin, “Space charge modules for PyHEADTAIL,” no. CERN-ACC-2016-0342, MOPR025. 6 p, Jul. 2016.
- [12] I. M. Kapchinskij and V. V. Vladimirkij, “Limitations of proton beam current in a strong focusing linear accelerator associated with strong space charge,” in *International Conference on High Energy Accelerators*, 1959, pp. 274–288.
- [13] F. J. Sacherer, “Rms envelope equations with space charge,” *IEEE Transactions on Nuclear Science*, vol. 18, no. 3, pp. 1105–1107, 1971.
- [14] W. Hardt, “On the Incoherent Space Charge Limit for Elliptic Beams,” *CERN ISR-INT-300-GS-66-2*, Jan. 1966.
- [15] R. L. Gluckstern, “Oscillation Modes in Two Dimensional Beams,” in *Proton Linear Accelerator Conference*, vol. C700928, 1970, p. 811.
- [16] E. Métral, “General formula to deduce the space charge tune spread from a quadrupolar pick-up measurement,” no. CERN-ACC-2016-0097, MOPR024. 4 p, Jul. 2016.
- [17] P. M. Lapostolle, “Quelques propriétés essentielles des effets de la charge d’espace dans les faisceaux continus,” CERN, Geneva, Tech. Rep. CERN-ISR-DI-70-36. ISR-DI-70-36, Aug. 1970.
- [18] D. Chernin, “Evolution of RMS beam envelopes in transport systems with linear X-Y coupling,” *Part. Accel.*, vol. 24, pp. 29–44, 1988.
- [19] M. Venturini and M. Reiser, “Self-consistent beam distributions with space charge and dispersion in a circular ring lattice,” *Phys. Rev. E*, vol. 57, pp. 4725–4732, 4 Apr. 1998.
- [20] M. Venturini and M. Reiser, “Rms envelope equations in the presence of space charge and dispersion,” *Phys. Rev. Lett.*, vol. 81, pp. 96–99, 1 Jul. 1998.
- [21] P. Zisopoulos, F. Antoniou, E. Hertle, A.-S. Muller, and Y. Papaphilippou, “Transverse Tunes Determination from Mixed BPM Data,” no. CERN-ACC-2015-289, TUPJE042. 4 p, 2015.
- [22] R. Bartolini and F. Schmidt, “SUSSIX: A computer code for frequency analysis of non-linear betatron motion,” 1998.
- [23] E. Métral, “Theory of coupled Landau damping,” *Part. Accel.*, vol. 62, no. CERN-PS-99-011-CA, 259. 14 p, Feb. 1999.
- [24] P. P. Bagley and D. L. Rubin, “Correction of transverse coupling in a storage ring,” in *Particle Accelerator Conference, 1989. Accelerator Science and Technology., Proceedings of the 1989 IEEE*, Mar. 1989, 874–876 vol.2.
- [25] S. Persichelli *et al.*, “Chromaticity Dependence of the Transverse Effective Impedance in the CERN Proton Synchrotron,” no. CERN-ACC-2015-337, MOPJE047. 4 p, 2015.